

Majorana-like fermion physics: Emergence of topologically protected vortical states in graphene interacting with an electromagnetic field

H. V. Grushevskaya* and George Krylov†

Belarusian State University, 4 Nezavisimosti Ave., 220030 Minsk, Belarus

(Dated:)

Within the framework of a quasi-relativistic model of graphene that admits topologically nontrivial Majorana-like quasiparticle excitations, appearance of such vortex states in the frequency dependencies of the complex dielectric permittivity of the system subjected to an external electromagnetic field has been examined. The vortex graphene states possess topological charges (flavours) being nonzero Zak phases. Interaction effects of Majorana-like modes have been qualitatively related to the formation of Fano resonances in the optical response. The constructed topological model of graphene may be considered as a toy model of three-flavour mass-neutrino oscillations.

PACS numbers: 72.80.Vp, 12.60.-i

Keywords: Majorana-like fermion, graphene, topologically protected vortical state, electromagnetic field.

I. INTRODUCTION

Majorana physics of high-energy interactions is currently actively searched for after obtained experimental evidence of the existence of non-zero masses in left-handed (LH) neutrinos. The neutrino masses change periodically (see [1] and references therein). There exist several scenarios for the origin of the three-flavour neutrino oscillations. The simplest explanation, which extends the Standard Model (SM) of Particle Physics, suggests a Majorana origin for neutrinos. The Majorana fields perform neutrino-electromagnetic-plasma coupling through the Higgs exchange in Early Universe. The right-handed (RH) field χ interacts with both a RH SM quark q_R and a mediator to SM gauge field \tilde{q} via a Yukawa interaction proportional to $\tilde{q}\bar{q}_R\chi$ [2, 3]. The scenario is based on the fact that the elusive RH particle χ is free due to the suppression of its interaction with other particles by CP symmetry. Such elementary particles are called sterile heavy leptons. The three-flavour neutrino oscillations are evidence of the fact that the Majorana mass term should disappear. It is assumed that the vanishing of the non-zero Majorana mass term with the subsequent transformation of the LH Majorana particles into Weyl ones occurs during the decoupling. Such neutrinos are

*Electronic address: grushevskaja@bsu.by

†Electronic address: krylov@bsu.by

called active ones. Instead of describing the decoupling stage, the mixing states of the LH active neutrinos with the sterile lepton are phenomenologically calculated by giving the observed pattern of masses and mixing in order to form a combination of both the sterile RH particle and the massless LH Weyl neutrinos [4]. The difficulty with this approach is that, along with the Majorana mass, the Yukawa interaction and, correspondingly, the sterile heavy leptons should disappear as well. The mechanism for the periodic alternation of the Majorana and Dirac mass spectra, referred to as the seesaw mechanism, is considered as one of the SM big puzzles. In another scenario, it is proposed to explain the neutrino mass spectrum through an electroweak-symmetry-breaking RH partner to the left-handed Weyl neutrino (see [5] and references therein). Having acquired a mass through Yukawa coupling, the sterile RH neutrino remains free due to CP symmetry, but periodically mixes with active LH massless Weyl neutrinos, providing them an apparent mass. However, the issue of Majorana physics inevitably arises after the addition of the right-handed Weyl neutrinos. The introduction of the RH neutrino is a model complication, but any complication can be viewed as a drawback, added to the same drawbacks as in the first scenario.

Majorana processes such as neutrinoless double beta decays (see [6] and references therein) are very rare events because of the TeV energy range. Until now, improvements to detector capabilities for rare decays have been focused on neutrino double-beta decays, which meet much more frequently than Majorana neutrinoless double-beta decays. Attempts to observe ultra-rare Majorana events are beyond the capabilities of current detectors [7]. Active neutrinos can oscillate into sterile neutrinos [8]. But, all unsuccessful search for the appearing sterile neutrino [9] points out that scenarios beyond the active-sterile mixing framework may be required.

Thus, in the absence of experimental power, the confirmation of theoretical predictions of Majorana physics is problematic.

Analogues of hypothetical elementary Majorana and Dirac-Weyl particles are invoked to explain topologically nontrivial quantum phases of strongly correlated many-body systems. Zero-dimensional Majorana modes of one-dimensional Kitaev chains are observed experimentally as the emergence of nonzero electron density at the ends of the atomic chains. Two-dimensional (2D) Majorana modes can be represented as two-dimensional vortices with a topological defect inside. However, theoretical predictions have significant discrepancies with experimentally observed optical and electrical properties of topological unconventional superconductors, and just as in high energy physics, the 2D Majorana modes remain elusive single-particle excitations in solid-state physics.

Generally speaking, massless fermions are chiral ones. After they acquire a mass, a revision of the chirality of the processes and subsequent search for the manifestations of chirality anomalies are required. Graphene is a strongly correlated many-electron system that is testified by the existence of correlation-

induced spin-charge separation for graphene states [10].

In this paper, we study a Majorana-like fermionic graphene model with topological subgap states and non-Abelian statistics. We will show that the Majorana-like fermions carry topological charge, and the law of conservation of topological charge allows only for interactions between zero-energy Majorana modes. However, this Majorana-like interaction manifests itself in a chiral anomaly. We demonstrate that the gapping of the Majorana electron band structure of graphene in magnetic fields leads to the expulsion of three Majorana-like modes to the first Landau level. This chiral anomaly is observed as Fano resonances of the complex graphene dielectric function at excitation near the Dirac valleys $K(K')$ of the graphene Brillouin zone; when the Majorana mass term disappears, the response to electromagnetic excitation of the electron density in flat regions near the M points of the graphene Brillouin zone oscillates. We aim to interpret this behavior as a seesaw mechanism within the framework of a toy Majorana-like fermion model of high-energy physics with three-flavour neutrino oscillations.

II. MAJORANA-LIKE PHYSICS OF GRAPHENE FERMIONS IN ELECTROMAGNETIC FIELDS

Graphene is a hexagonal layer of carbon atoms with one atom thick. Its two electrons per primitive rhombic unit cell are located on the trigonal sublattices A and B of the hexagonal lattice. A Landau level with energy at a point or valley $K(K')$ named as the Dirac point of graphene Brillouin zone is half-filled in neutral graphene. Fig. 1a shows the graphene Brillouin zone. Therefore, the wave functions ψ_{AB} and ψ_{BA}^* of graphene charge carriers are attributed to the wave function of graphene sublattices A and B , respectively; here $*$ is complex conjugation. The graphene wave function $(\psi_{AB}, \psi_{BA}^*)^T$ is the wave of electron-hole pair being resident in graphene, where T is the transposition operation. Since the electron-hole pair is simultaneously its own antiparticle, a model with fermions similar to Majorana ones is necessary to describe graphene. Such a quasi-relativistic graphene model has been derived in [18] as a consequent account of the effect of relativistic exchange interactions. The model is grounded on truly secondary quantized relativistic consideration of the problem within the known Dirac-Hartree-Fock self-consistent field approximation. In subsequent publications [16, 19, 20] it has been established that the model admits a form as Majorana-like system of equations as well as two-dimensional Dirac-like equation with an additional ‘‘Majorana-force correction’’ term [16].

The Hamiltonian of Majorana-like fermions in an external electromagnetic field reads [11, 16, 17]

$$\left[c\vec{\sigma}_{2D}^{BA} \cdot \left(\vec{p}_{AB} - \frac{e}{c}\vec{A} \right) - \widetilde{M}_{AB} \left(\vec{p}_{AB} - \frac{e}{c}\vec{A} \right) \right] |\psi_{AB}\rangle = ic \frac{\partial}{\partial t} |\psi_{BA}^*\rangle, \quad (1)$$

$$\left[c\vec{\sigma}_{2D}^{AB} \cdot \left(\vec{p}_{BA}^* + \frac{e}{c}\vec{A} \right) - \left(\widetilde{M}_{BA} \left(\vec{p}_{BA} - \frac{e}{c}\vec{A} \right) \right)^* \right] |\psi_{BA}\rangle = -ic \frac{\partial}{\partial t} |\psi_{AB}^*\rangle. \quad (2)$$

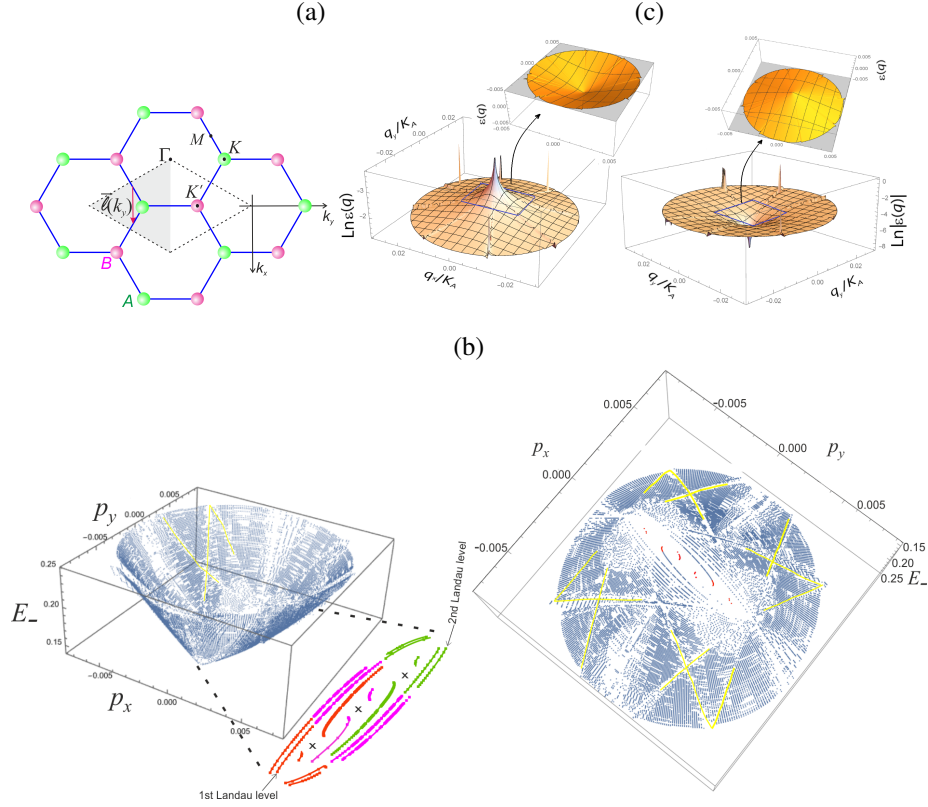


FIG. 1: (a) Graphene hexagonal lattice of Brillouin zone. A change $\vec{\gamma} [\vec{l}(k_y)]$ in the flux of non-Abelian gauge field along the paths $\vec{l}(k_y)$ defines Wilson loops. A rhombic first Brillouin zone (BZ) of the honeycomb lattice consisting of two triangular sublattices A (green) and B (red) is labeled with a dashed line. High-symmetry points are Γ , $K(K')$, M . Occupied half-BZ is gray shaded. A reference point of coordinates (k_x, k_y) is in Γ . (b) A valence (conduction) band of Majorana fermions in graphene subjected to an electromagnetic field: (left) side view and (right) top view. The yellow lines provide a guide to the eye for the 4 conical and 4 pseudo-Dirac one-dimensional forbidden zones. The excited Majorana modes are painted in red color. The figure, bottom and Inset in it illustrate the cyclotron gap (the first Landau level) appearing due to the Landau quantization and a splitting of the shifted Majorana zero-energy mode entering the quantized spectrum of graphene. The inset shows the bottom of the perturbed band up to and including the 2nd Landau level; the three discontinuities in the anomalous dispersion energy levels curves are designated by “crosses”. The three excited Majorana modes with the corresponding two Landau levels are colored in orange, magenta, and green. (c) The graphene bandstructure non-perturbed by external field action.

Here \widetilde{M}_{AB} (\widetilde{M}_{BA}) is an unconventional Majorana-like mass term for a quasiparticle in the sublattice $A(B)$; $\vec{\sigma}_{2D}^{AB} = \Sigma_{BA} \vec{\sigma}_{2D} \Sigma_{AB}^{-1}$, $\vec{\sigma}_{2D}^{BA} = \Sigma_{AB} \vec{\sigma}_{2D} \Sigma_{BA}^{-1}$, $\vec{\sigma}_{2D} = \{\sigma_x, \sigma_y\}$ is the 2D vector of the Pauli matrixes; $\vec{p}_{2D}^{AB} = \Sigma_{AB} \vec{p} \Sigma_{AB}^{-1}$, $\vec{p}_{2D}^{BA} = \Sigma_{BA} \vec{p} \Sigma_{BA}^{-1}$, $\vec{p} = \{p_x, p_y\}$ is the 2D momentum operator, Σ_{AB} and Σ_{BA} are relativistic quantum-exchange operators for sublattices A, B respectively; \vec{A} is a vector-potential of electromagnetic field, c is the speed of light, e is the electron charge. The Majorana-like mass terms \widetilde{M}_{BA}

and \widetilde{M}_{AB} are determined as

$$\widetilde{M}_{BA} = \alpha i^2 \Sigma_{BA} \Sigma_{AB} - \hbar c (\vec{\sigma}^{AB} \cdot \vec{p}^{BA}) \vec{\sigma}^{AB} \cdot (\vec{K}_B^{BA} + \vec{K}_A^{BA}), \quad (3)$$

$$\widetilde{M}_{AB} = \alpha i^2 \Sigma_{AB} \Sigma_{BA} - \hbar c (\vec{\sigma}^{BA} \cdot \vec{p}^{AB}) \vec{\sigma}^{BA} \cdot (\vec{K}_B^{AB} + \vec{K}_A^{AB}) \quad (4)$$

where α is an arbitrary constant, $\vec{K}_A^{BA} = \Sigma_{BA} \vec{K}_A \Sigma_{BA}^{-1}$ ($\vec{K}_B^{BA} = \Sigma_{BA} \vec{K}_B \Sigma_{BA}^{-1}$), $\vec{K}_A^{AB} = \Sigma_{AB} \vec{K}_A \Sigma_{AB}^{-1}$ ($\vec{K}_B^{AB} = \Sigma_{AB} \vec{K}_B \Sigma_{AB}^{-1}$), \vec{K}_A and \vec{K}_B denote the valleys \vec{K} and \vec{K}' , $\hbar = h/(2\pi)$, h is the Planck constant. You can see that \widetilde{M}_{BA} (\widetilde{M}_{AB}) is comprised by the two terms being the proper Majorana mass term which is proportional to $\Sigma_{BA} \Sigma_{AB}$ ($\Sigma_{AB} \Sigma_{BA}$) and the coupling

$$V_{o-v} = -\hbar c (\vec{\sigma}^{AB} \cdot \vec{p}^{BA}) \vec{\sigma}^{AB} \cdot (\vec{K}_B^{BA} + \vec{K}_A^{BA}) \quad (5)$$

between orbital and valley currents. In what follows we vary the parameter α and omit the symbol $2D$ in designations of the transformed vector of $2D$ Pauli matrixes. The presence of the coupling between orbital and valley current means that the problem (1)–(2) is effectively many-body one due to account of electron-hole correlations.

The relativistic exchange operator for the tight-binding approximation and accounting of nearest lattice neighbors is given by its action on secondary quantized wave functions on sublattices $A(B)$ of the system [18–20] in the following form:

$$\begin{aligned} & \Sigma_{rel}^x \begin{pmatrix} \widehat{\chi}_{-\sigma_A}^\dagger(\vec{r}) \\ \widehat{\chi}_{\sigma_B}^\dagger(\vec{r}) \end{pmatrix} |0, -\sigma\rangle |0, \sigma\rangle \\ &= \begin{pmatrix} 0 & \Sigma_{AB} \\ \Sigma_{BA} & 0 \end{pmatrix} \begin{pmatrix} \widehat{\chi}_{-\sigma_A}^\dagger(\vec{r}) \\ \widehat{\chi}_{\sigma_B}^\dagger(\vec{r}) \end{pmatrix} |0, -\sigma\rangle |0, \sigma\rangle, \end{aligned} \quad (6)$$

with

$$\Sigma_{AB} \widehat{\chi}_{\sigma_B}^\dagger(\vec{r}) |0, \sigma\rangle = \sum_{i=1}^{N_v N} \int d\vec{r}_i \widehat{\chi}_{\sigma_B}^\dagger(\vec{r}_i) V(\vec{r}_i - \vec{r}) |0, \sigma\rangle \quad (7)$$

$$\times \Delta_{AB} \langle 0, -\sigma_i | \widehat{\chi}_{-\sigma_A}^\dagger(\vec{r}_i) V(\vec{r}_i - \vec{r}) \widehat{\chi}_{-\sigma_B}(\vec{r}_i) |0, -\sigma_i\rangle,$$

$$\Sigma_{BA} \widehat{\chi}_{-\sigma_A}^\dagger(\vec{r}) |0, -\sigma\rangle = \sum_{i'=1}^{N_v N} \int d\vec{r}_{i'} \widehat{\chi}_{-\sigma_A}^\dagger(\vec{r}_{i'}) V(\vec{r}_{i'} - \vec{r}) |0, -\sigma\rangle \quad (8)$$

$$\times \Delta_{BA} \langle 0, \sigma_{i'} | \widehat{\chi}_{\sigma_B}^\dagger(\vec{r}_{i'}) V(\vec{r}_{i'} - \vec{r}) \widehat{\chi}_{\sigma_A}(\vec{r}_{i'}) |0, \sigma_{i'}\rangle. \quad (9)$$

Here $V(\vec{r})$ is the three-dimensional (3D) Coulomb potential, summation is performed on all lattice sites and number of electrons, the interaction (2×2) -matrixes Δ_{AB} and Δ_{BA} are gauge fields (or components of a gauge field). Vector-potentials for these gauge fields are introduced by the phases α_0 and $\alpha_{\pm, k}$, $k = 1, 2, 3$ of $\pi(p_z)$ -electron wave functions $\psi_{p_z}(\vec{r})$ and $\psi_{p_z, \pm \delta_k}(\vec{r})$ attributed to a given lattice site and its three nearest

neighbors (see details in [20]). The definition of these three non-Abelian gauge fields was stipulated by a requirement of reality of eigenvalues of the Hamiltonian operator as gauge conditions. The operator of relativistic exchange gains an additional implicit \vec{p} -dependence upon momentum in the case of non-zero values of gauge fields [11].

III. CHIRALITY ANOMALIES AND DECONFINEMENT OF MAJORANA-LIKE MODES WITH FANO-RESONANCE COUPLING

Let the multiplier

$$m_{precession} \equiv \vec{\sigma}^{AB} \cdot (\vec{K}_B^{BA} + \vec{K}_A^{BA}) \quad (10)$$

entering the spin–valley-current coupling V_{o-v} (5) be considered as vanishing

$$\vec{\sigma}^{AB} \cdot (\vec{K}_B^{BA} + \vec{K}_A^{BA}) = 0. \quad (11)$$

In magnetic fields, since discrete Landau energy levels arise the perturbed graphene bandstructure is gapped (see Fig. 1b). Three excited Majorana-like modes as the three anomalies of energy dispersion emerge in the vicinity of the valley for the graphene model with a nonzero Majorana mass term $\Sigma_{BA}\Sigma_{AB}$ ($\Sigma_{AB}\Sigma_{BA} \neq 0$) (see Fig. 1b). At zero magnetic fields, the unperturbed graphene band touches with the unperturbed graphene conduction in the Dirac point as Fig. 1c shows. These three Majorana modes are revealed in the frequency dependence of the complex optical conductivity when $\Sigma_{BA}\Sigma_{AB}$ ($\Sigma_{AB}\Sigma_{BA} \neq 0$). The three anomalous dispersions correspond to the three peaks "A1", "A2", and "A3" of the dielectric function (see Fig. 2a).

The optical response of the Majorana-like graphene model deviates significantly from the theoretically predicted constant behavior of its optical conductivity in the pseudo-Dirac theory. In the ultraviolet range, a broad band with a maximum of 4.74 eV (5.5×10^4 K) is observed, being asymmetric as a Fano resonance (see Fig. 2a). For massless graphene fermions of the Majorana type, these three peaks "A1", "A2", and "A3" corresponding to the three anomalous dispersions degenerate into the one peak labeled by "A". Since the chiral anomalies vanish, the chirality of the model is restored, and therefore the optical conductivity becomes, on average, equal to $0.25 G$, as for graphene fermions of pseudo-Dirac type. Here $G/2$ is the quantum of minimal conductivity. It means that magnetic fields lift the degeneracy of the Majorana-type bandstructure (see Fig. 1b).

For the topologically nontrivial pseudo-Majorana graphene model, a topological defect is located at the

Dirac point $K(K')$; charge carriers, bypassing this defect, acquire a nonzero phase called the Zak phase as

$$Q = -ie \oint_{C_{BZ}} \frac{d\vec{k}}{(2\pi)^d} \cdot \left\langle u_{\vec{k}}(\vec{r} + \vec{R}(t_0 + \epsilon)) \left| \frac{\partial}{\partial \vec{k}} \right| u_{\vec{k}}(\vec{r} + \vec{R}(t_0)) \right\rangle, \quad \epsilon \rightarrow 0 \quad (12)$$

where C_{BZ} is a path which is equivalent to a closed loop of d -dimensional Brillouin zone due to crystal symmetry, $u_{\vec{k}}(\vec{r} + \vec{R}(t_0))$ is a Bloch function, $t_0, t_0 = 0$ is a time. The physical meaning of the Zak phase Q consists in the emergence of electric polarization (nonzero dipole moment) $\vec{d} = e\vec{r}$ [12, 13] because the operator $i \frac{\partial}{\partial \vec{k}}$ is a position operator \vec{r} . The transition dipole moment $\langle \vec{K} | \vec{r} | \vec{K} + \vec{q} \rangle, \vec{q} \rightarrow 0$, in the vicinity of the Dirac point is nonzero as the law of topological-charge conservation forbids its change.

The behavior of the real part of the complex Hall conductivity remains qualitatively the same, whereas the imaginary contribution of the complex Hall conductivity to the graphene dielectric function has three plasmon modes (three regions of negative values) when $\Sigma_{BA}\Sigma_{AB} (\Sigma_{AB}\Sigma_{BA}) \neq 0$, or one in the zero-Majorana-mass case (see Fig. 2b). These plasmons are oscillations of graphene quasiparticle excitations, the annihilation of which is prevented by the polarization of the graphene electron density with the dipole moment \vec{d} per one electron–hole pair. It means that bound charge carriers are always present in the graphene valleys. Thus, topological defects effectively transfer a portion of charge carriers from the valence band to the conduction band. In contrast to the graphene Majorana-like fermions, pseudo-Dirac graphene charge carriers are absent at $K(K')$ in the low-frequency limit, $\omega_0 \rightarrow 0$.

The wave functions of an electron and a hole, ψ_e and ψ_h of a non-topological electron–hole pair and, correspondingly, a wave Ψ_{e-h} of the pair acquire Pancharatnam–Berry phases [14, 15] in a magnetic field \vec{B} with the vector-potential \vec{A} as

$$\begin{aligned} \Psi_{e-h}(\vec{A}) &= \psi_e \exp \left\{ -\frac{ie}{\hbar c} \oint_{C_e} d\vec{r}_e \cdot \vec{A}(\vec{r}_e) \right\} \psi_h \exp \left\{ -\frac{ie}{\hbar c} \oint_{C_h} d\vec{r}_h \cdot \vec{A}(\vec{r}_h) \right\} \\ &= \Psi_{e-h}(0) e^{i(\gamma_e + \gamma_h)} \end{aligned} \quad (13)$$

where $C_e (C_h)$ is a loop electron (hole) path, $\gamma_e (\gamma_h)$ is the electron (hole) Berry phase. The wave functions of an electron and a hole, ψ_e^T and ψ_h^T , of a topologically protected pair acquire Berry phases, γ_e^T and γ_h^T , opposite in sign and equal in magnitude, $\gamma_e^T = -\gamma_h^T$, as the dipole moment \vec{d} is attributed to the topological electron–hole pair with a wave function Ψ_{e-h}^T . The wave function Ψ_{e-h} of the topologically protected electron–hole pair does not change, because

$$\begin{aligned} \Psi_{e-h}^T(\vec{A}) &= \psi_e^T \exp \left\{ -\frac{ie}{\hbar c} \oint_{C_{e,T}} d\vec{r}_e \cdot \vec{A}(\vec{r}_e) \right\} \psi_h^T \exp \left\{ -\frac{ie}{\hbar c} \oint_{C_{h,T}} d\vec{r}_h \cdot \vec{A}(\vec{r}_h) \right\} \\ &= \Psi_{e-h}^T(0) e^{i(\gamma_e^T + \gamma_h^T)} \equiv \Psi_{e-h}^T(0) \end{aligned} \quad (14)$$

where $C_{e,T} (C_{h,T})$ is a closed loop electron (hole) path around the topological defect, $C_{e,T} = C_{h,T}$, $\gamma_e (\gamma_h)$ is the Berry phase for the electron (hole) belonging to the topological pair. Eq. (14) explains the conservative

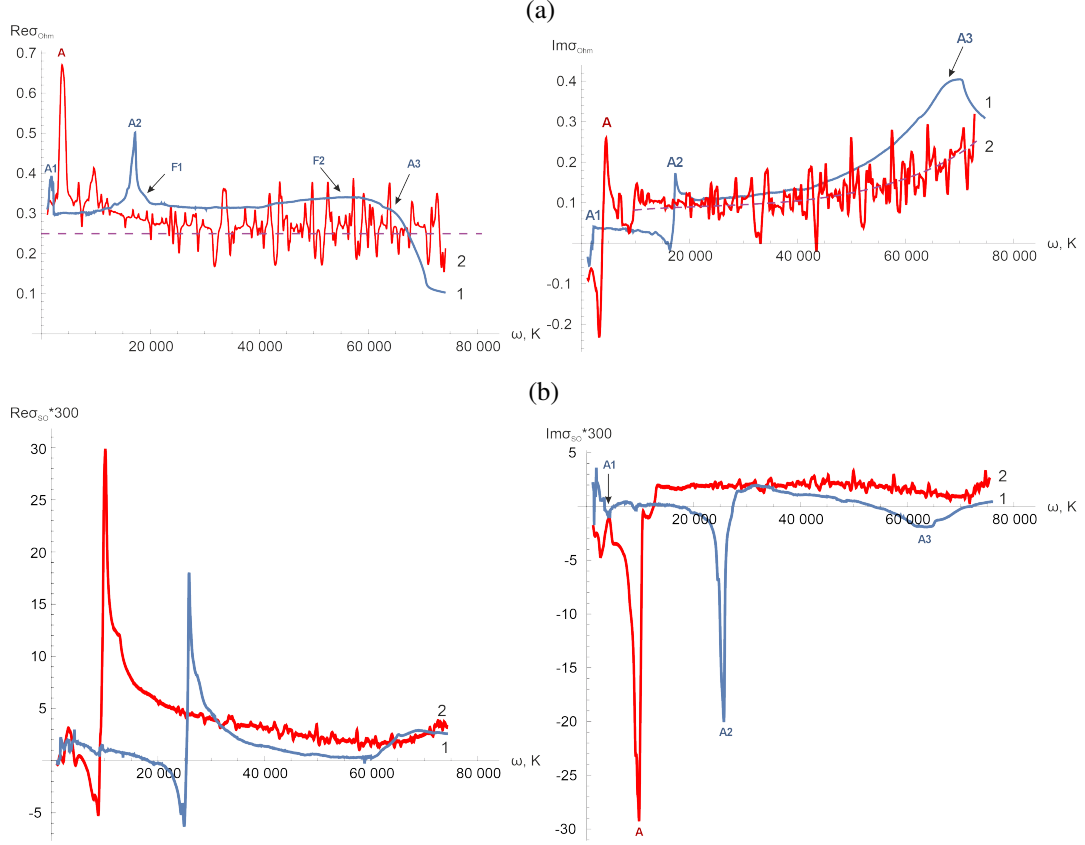


FIG. 2: Real (left) and imaginary (right) of optical (a) and Hall (b) complex conductivity for graphene Majorana-like fermion model with (blue curves “1”) and without (red curves “2”) the mass term; the dashed line is the optical conductivity of pseudo-Dirac graphene model. “F1” and “F2” denote Fano resonances, “A” and “A $_i$ ”, $i = 1, 2, 3$ denote degenerated and non-degenerated Majorana-like modes.

behavior of the real part of the Hall conductivity with respect to the phase accumulation of electrons and holes composing topological electron–hole pairs in a magnetic field \vec{B} (see Fig. 2b). Thus, the Berry phase is not a topological invariant of the pseudo-Majorana graphene model.

Two Fano resonances (broad asymmetric bands of $\Re e \sigma_{\text{Ohm}}$), denoted as “F1” and “F2” in Fig. 2a, are evidence of the fact that the Majorana modes are weakly coupled and interfere with a fourth background process. The impact of the non-zero Majorana mass term, \tilde{M} gives rise the Majorana-modes coupling as repulsion of the Majorana-like modes with same sign of their topological charges from each other and, hence, \tilde{M} behaves as a certain interaction.

Further, a mechanism of the Majorana-modes flavour interaction and an origin of the fourth background process are elaborated.

IV. INTERVALLEY-PRECESSION COUPLING MAJORANA-LIKE MODES AS A TOPOLOGICAL TOY MODEL MECHANISM OF NEUTRINO OSCILLATIONS

A. Emerging Majorana-like vortical states

In the absent of the electromagnetic field, defects as core of vortices remain in the Dirac point. As one can see in Fig. 3a, the contour plots of the graphene energy electron valent (conduction) and hole conduction (valent) bands are vortexed in the neighborhood of $K(K')$ and the feathering of the vortex consists of an infinitely many vortices of varying widths, called vortex sleeves. Each vortex sleeve is located in a limited range of wave vector values. Such discreteness is an attribute of quantization of the vortex sleeve. Due to the law of conservation of angular momentum, both left- and right-twisting vortices are generated. Due to the law of conservation of the helicity of massless charge carriers, the replacement $\vec{k} \rightarrow -\vec{k}$ produces a vortex LH hole (electron) conductivity band from the RH electron (hole) valent band.

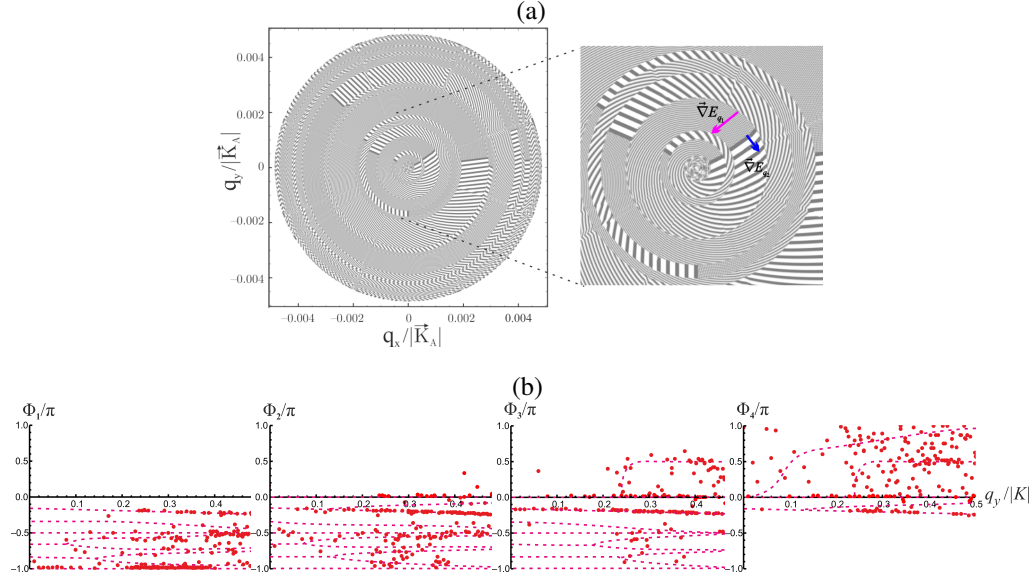


FIG. 3: (a) A spin-orbit texture of the bands on momentum scales $q/K = 0.002$ in contour plots and a model of intervalley-precession coupling Majorana-like modes (in inset to (a)). (b) Non-Abelian phases Φ_1, \dots, Φ_4 of the Wilson-loop eigenvalues in the units of π at non-zero gauge fields.

The vortical graphene states are topological ones as at bypass around the vortex core, electrons and holes acquire nonzero discrete Zak phases Q (see Fig. 3b). These Zak phases at high wave numbers q , $\vec{q} = \vec{k} - \vec{K}$ form the cyclic group Z_8 with a generator $-\frac{\pi}{4}$ or $\frac{\pi}{4}$ for electrons or holes at sufficiently high wave numbers q as

$$Q = \mp \frac{n\pi}{4}, \quad n = 0, 1, \dots \quad (15)$$

where the Q are called topological charges or flavours. To reconcile the presence of topological charges (15) with the electron–hole symmetry one should assign zero value to whole graphene topological charge

$$Q_{graphene} = 0. \quad (16)$$

Three resonances which emerge in the optical graphene response $\Re e \sigma_{Ohm}$ (the real part of the ohmic contribution to the optical conductivity) at $\Sigma_{BA}\Sigma_{AB}$ ($\Sigma_{AB}\Sigma_{BA}$) $\neq 0$ and are shown in Fig. 2a, are the direct evidence of existence for three topologically non-trivial Majorana-like modes with different nonzero topological charges, for example, such as

$$Q_n = \mp \frac{(n+1)\pi}{4}, \quad n = 1, 2, 3. \quad (17)$$

Since a total topological charge $Q_{sum} = \sum_{i=1}^3 Q_i$ of the Majorana-like mode configuration is non-multiple to 2π and equal to

$$Q_{sum} = \frac{\mp 9\pi}{4} \quad (18)$$

the law of topological-charge conservation prevents the decay of the Majorana vortical states through topologically trivial electron–hole annihilation.

In the massless case ($\tilde{M} = 0$), the three resonances are degenerated into one as the comparison of the simulation results for graphene optical response show for the case with and without mass term $\Sigma_{BA}\Sigma_{AB}$ ($\Sigma_{AB}\Sigma_{BA}$) demonstrates (make a comparison between the curves “1” and “2” in Fig. 2a). It testifies that the $\Sigma_{BA}\Sigma_{AB}$ ($\Sigma_{AB}\Sigma_{BA}$) describes interaction of the Majorana modes with different topological charges (flavours) with each other by the following mechanism. In analogy as electromagnetic interaction pushes out topological defects (vortex cores) in the neighbourhood of the 1st Landau level, the coupling $\Sigma_{BA}\Sigma_{AB}$ ($\Sigma_{AB}\Sigma_{BA}$) creates color energy gap $E_{g,Q_n}(q_n)$, $\vec{q}_n = \vec{k}_n - \vec{K}$ of the graphene bandstructure that forbides the presence of Majorana modes in the $K(K')$ point and positions the vortex cores in non-coinciding points \vec{q}_n , $n = 1, 2, 3$ of the Brillouin zone (see Fig. 1b). The Q -flavour interactions may proceed before a moment when external electromagnetic field pushes out the Majorana-like modes into vicinity of the 1st Landau level and visa versa the flavour Majorana-like vortical modes may be redistributed on the discrete Landau levels after the impact of the electromagnetic field \vec{A} on p_z electrons gives rise the flavour interactions. Resonances in the system of coupled oscillators in an external field are called Fano resonances. The Fano-like resonances being observed in the real part of σ_{Ohm} is signature of the graphene vortical states which form a system of three coupled oscillators in an external field.

B. Topological-charge affect on quantum interference

The phase of the wave function of a graphene charge carrier acquires an additional Berry phase ϕ_B upon bypassing any defect, including a topological one, in the magnetic field \vec{B} of electromagnetic radiation with the vector potential \vec{A} . If the defect is not topological one, quantum interference of charge carriers with different phases would lead to a change (decrease) in the intensity of the optical response, and the magnitude of this change depends on the frequency ω of \vec{A} . The topological charge conservation law prohibits the effect of quenching of out-of-phase waves that carry non-zero topological charge, the last explains the monotonic frequency dependence of the graphene conductivity at $\tilde{M} \neq 0$ (see Fig. 2).

The observable merging of three Majorana resonances with the total topological charge Q_{sum} (18) into a single one when $\tilde{M} = 0$ (see Figs. 1b and 2a) means that the Majorana modes are degenerate without the flavour interactions. The topological charges of all three flavour Majorana modes that constitute this degenerate mode are located at the same point (the Dirac point $K(K')$). However, generally speaking, the topological charge $Q_d(K)$ of the degenerate Majorana mode residing at $K(K')$ must vanish in accordance with the zero value of the graphene topological charge Q_{graphene} (16). The topological charge $Q_d(K)$ becomes zero under the condition that a compensating topological countercharge $Q_0(K)$, equal to $Q_0(K) = -Q_{\text{sum}}$, is located at the merging point of the cores of the flavour Majorana modes (at each point $K(K')$ of reciprocal space), so that

$$Q_d(K) = Q_0(K) + Q_{\text{sum}} = 0 \text{ for } \tilde{M} = 0. \quad (19)$$

The ant flavour $Q_0(K)$ satisfying to the condition (19) must be always resident in the graphene valley because the requirement (16) holds.

Since in the absence of flavour interaction at $\tilde{M} = 0$ the all flavour vortex cores degenerate into a single flavourless Majorana-like zero-energy mode, and the electromagnetic field \vec{A} with Abelian statistics is insensitive to topological charge, flavourless vortices as coherent quantum structures must interfere with each other as quasiparticle excitations with different phases. Since the Berry phase ϕ_B , acquired by a graphene charge carrier upon bypassing a topological defect in the magnetic field \vec{B} of electromagnetic radiation, is added to the phase of its wave function, the interference pattern must oscillate with the variation of the frequency ω of \vec{A} . This explains the observed oscillations of $\Re e \sigma_{Ohm}(\omega)$ at $\tilde{M} = 0$ (see the curves “2” in Fig. 2).

We note that the oscillation amplitude of the optical conductivity σ_{Ohm} varies with increasing frequency ω of the applied field \vec{A} . This occurs due to the growth of the Majorana mode feathering through the formation of new non-overlapping vortex sleeves. Then, one can infer from this that each new sleeve

contributes an additional Berry phase ϕ_p to the wave function of the Majorana-like vortical state. To prove this, let us consider how the gradient $\vec{\nabla}E_q$ of the energy dispersion E_q varies along the vortex sleeve. The vorticity of graphene charge carrier states is revealed as a values drop of $\vec{\nabla}E_q$ from $\vec{\nabla}E_{q_1}$ to $\vec{\nabla}E_{q_2}$ with a 90° rotation of the vector $\vec{\nabla}E_q$ along the vortex sleeve in the direction away of the sink (vortex funnel) (see Fig. 3a) and

$$\vec{\nabla}E_{q_2} \perp \vec{\nabla}E_{q_1}, \quad \vec{\nabla}E_{q_2} \ll \vec{\nabla}E_{q_1} \quad (20)$$

where $\vec{\nabla} = \frac{\partial}{\partial \vec{q}}$. The change in the direction of the gradient $\vec{\nabla}E_q$ entails a reorientation of the spin of the massless charge carrier, because chiral symmetry always aligns its spin along the direction of motion. According to Fig. 1a, since electron-hole symmetry admits the energy levels E_{q_1} and E_{q_2} belonging to the electron (hole) and hole (electron) bands and the $\frac{\pi}{2}$ -angle turn is equivalent to $\frac{\pi}{6}$ due to the hexagonal symmetry, respectively, the quantum exchange can perform a transfer of the electron (hole) from a valley $K_{A_1}(K'_{B_1})$ into a valley $K_{A_2}(K'_{B_2})$ through both the Dirac $K'_B(K_A)$ and M points at transition between the energy levels E_{q_1} and E_{q_2} under an external affect. The process of alternating transition of an electron (hole) from one trigonal sublattice $A(B)$ to another $B(A)$ and back to $A(B)$ must be accompanied by a periodic change in spin direction. Such a process is called precession. The precession process is analogous to the bending of the trajectory of an electric charge in a magnetic field \vec{B} due to the electron–hole symmetry. Therefore, just as in the case of bypassing a topological defect in a magnetic field \vec{B} , the graphene charge carriers precessing along the j -th sleeve of the vortex acquire an additional Berry phase $\phi_{p,j}$, $j = 1, 2, \dots$. Since the sleeves do not coincide and their widths vary, $\phi_{p,i} \neq \phi_{p,j}$, $i \neq j$. The fact that with increasing frequency ω the Berry phase becomes different, taking the value of $\phi_B + \sum_{k=1}^j \phi_{p,k}$, explains the observed aperiodic variation of the interference pattern with increasing ω (see Fig. 2).

We note (see the curves “2” in Fig. 2a) that σ_{Ohm} value oscillates in the vicinity of half the graphene conductivity quantum of $0.25G$ (the conductivity quantum or minimal graphene conductivity is equal to $0.5G$, $G = \frac{e^2}{h}$). The value of $0.25G$ is the optical conductivity of the topologically trivial pseudo-Dirac model. Such behaviour confirms the assumption on the existence of a 4th flavour Q_0 not associated with any physical Majorana-like mode. Thus, the oscillations of graphene optical conductivity at $\tilde{M} = 0$, arising due to the existence of the topological anticharge $Q_0 = -\frac{\pi}{4}$ in our model, disappear due to the removal of degeneracy of the Majorana-like vortex cores by $\Sigma_{BA}\Sigma_{AB} \neq 0$ ($\Sigma_{AB}\Sigma_{BA} \neq 0$). The value $Q(q_i)$, $i = 0, \dots, 3$ of the topological charge being pushed out from the graphene valley to the point $\vec{k}_i = \vec{q}_i + \vec{K}$ of the Brillouin zone tends to $Q_i(0)$ at an infinitesimally small Majorana term, $\tilde{M} \rightarrow 0$. It means that according to the expression (19) the total topological charge Q_{total} of the flavour Majorana-like modes tends

to the following value:

$$Q_{total} = \sum_{i=0}^3 Q(q_i) \rightarrow \sum_{i=0}^3 Q_i(K) = Q_d(K) = 0 \text{ for } \tilde{M} \rightarrow 0 \quad (21)$$

and, correspondingly, the topological charges $Q_i(K)$, $i = 0, \dots, 3$ accumulated in $K(K')$ are completely pushed out from the graphene valley. Since the topological antidefect (antiflavour Q_0) can coexist with the topological defect (flavour Q_i , $i = 1, 2, 3$) only at the Dirac point $K(K')$ due to the chiral symmetry, the anti-Majorana state with the topological charge $Q(q_0)$ becomes unstable or unphysical and, correspondingly, the topological charge conservation law must prevent the quantum interference of the physical Majorana-like states with the flavour $Q(q_i)$, $i = 1, 2, 3$ as confirmed by the non-oscillating behaviour of the calculated optical graphene conductivity at $\Sigma_{BA}\Sigma_{AB} \neq 0$ ($\Sigma_{AB}\Sigma_{BA} \neq 0$). However, the behaviour of $\Re \sigma_{Ohm}$ becomes kink-like at high frequencies ω when the flavour Dirac cone bands begin to overlap and then mix (see the curve “1” in Fig. 2a, left). It is evidence of the fact that the presence of antiflavour electron (flavour hole) Majorana vortical states can give rise to this quenching of the Majorana waves at high energies ($\hbar\omega$).

Further, let us explore the origin of such flavour electron (antiflavour hole) Majorana-like vortical states to which the antiflavour (flavour) topological defects are admixed.

C. Chiral-symmetry recovery

Under an assumption of unchanged phases of the p_z electron wave functions (zero gauge fields when the interaction (2×2) -matrices Δ_{AB} ($\Delta_{BA}=1$), two $\Sigma_{BA}\Sigma_{AB}$ ($\Sigma_{AB}\Sigma_{BA}$) eigenvalues $M_i^{(0)}(q)$ ($-M_i^{(0)}(q)$), $i = 1, 2$ depending on $\vec{q} = \vec{k} - \vec{K}_A$ ($\vec{q} = -\vec{k} - \vec{K}_B$), are functions with saddle-type singular points residing in the graphene valleys; moreover, outside the valley one of the eigenvalues exceeds the other by two orders of magnitude (see Fig. 4a).

The electron–hole symmetry of massless graphene charge carriers, forbidding a change in their chirality, turns an electron (hole) into a hole (electron) upon reversal of the direction of the vector \vec{q} , $\vec{q} \rightarrow -\vec{q}$. According to Fig. 4a, outside the Dirac point, due to preservation of sign under the substitution $\vec{q} \rightarrow -\vec{q}$, the mass eigenvalue $M_i^{(0)}(q)$, $i = 1, 2$ violates chiral symmetry and, correspondingly, electron–hole pairs annihilate, destroying the feathering of the vortex cores upon the transition from one “wing” (“antiwing”) of the saddle to the opposite one. Thus, in the absence of gauge fields, the chiral Majorana modes outside the valley are unstable and can exist only at zero energy.

When the gauge fields are non-zero, the only one ($M_1(q)$) of two eigenvalues $M_1(q)$ and $M_2(q)$ of the Majorana-like term $\Sigma_{BA}\Sigma_{AB}$ ($\Sigma_{AB}\Sigma_{BA}$) remains a saddle, and the span of its “wings” sharply decreases

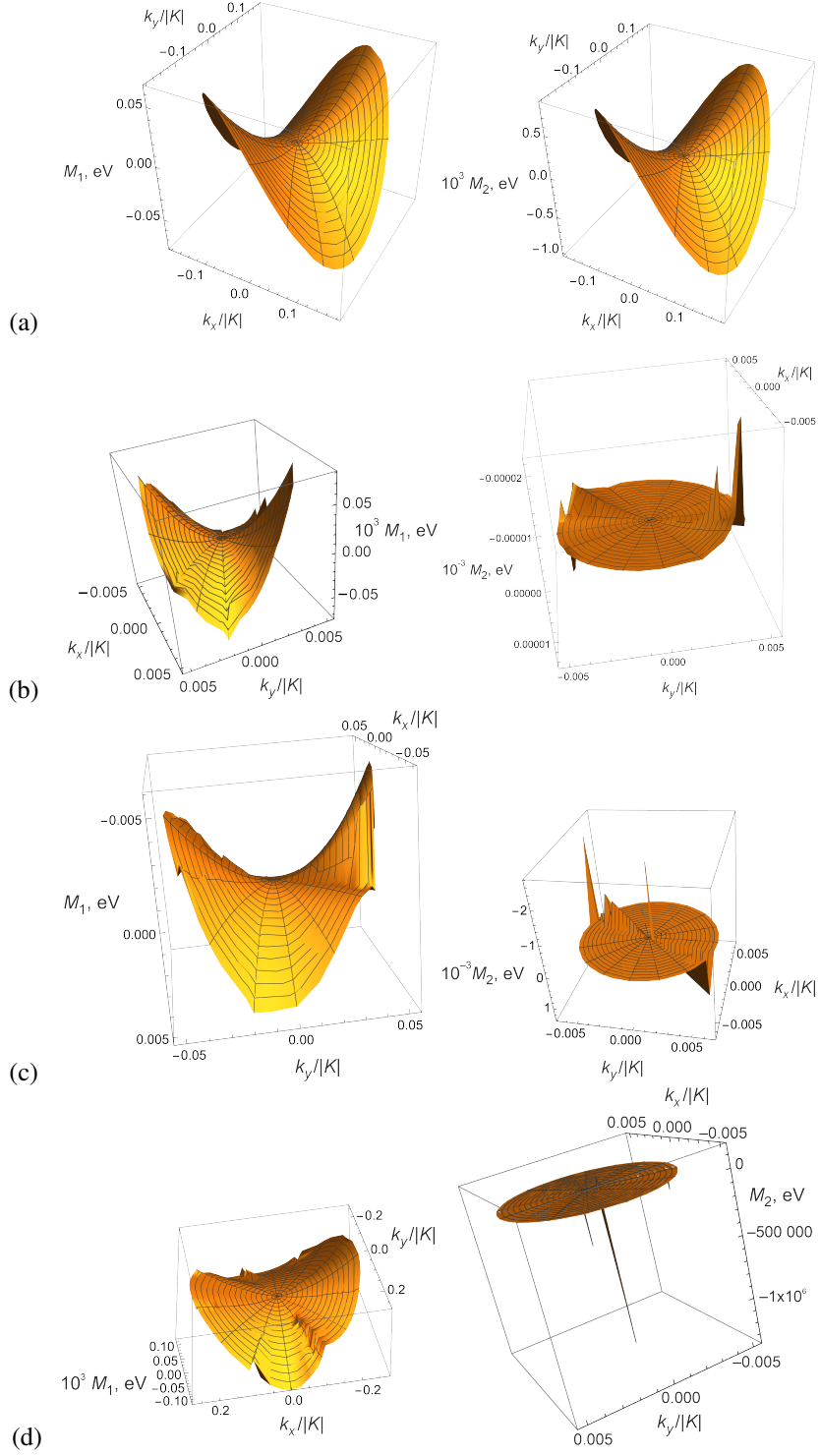


FIG. 4: Two eigenvalues, M_1 and M_2 , of the Majorana mass term at zero (a) and non-zero (b–d) gauge fields, without spin-valley current coupling (b), and with small (c) and large (d) spin-valley current coupling.

(see Fig. 4b):

$$M_1(q) \ll M_1^{(0)}(q), q > 0 \quad (22)$$

and, correspondingly, the feathering of one of the two possible vortex pairs always annihilates. Another eigenvalue $M_2(q)$ flattens (see Fig. 4b) so that the “antiwings” of the saddle vanish, and three mass resonances $M_r(q_i)$, $i = 1, 2, 3$ grow on one of the rudiments of the “wings”. Since the vortex-core energy E_0 is zero, the mass resonances give rise to a flavoured energy gap $E_g(q_i)$, $i = 1, 2, 3$ of the graphene bandstructure as

$$E_g(q_i) = E_0 + M_r(q_i), i = 1, 2, 3 \quad (23)$$

and the three flavour Dirac cones at the points q_i , $i = 1, 2, 3$ arise (see Fig. 1b). The topological-charge-conservation law (21) admits only the simultaneous coexistence of the three mass resonances and, in this sense, the three mass resonances give rise to an integral indivisible system of three coupled Majorana-like modes which reside in different non-overlapping vicinities of the Dirac point. This is the cause of the emergence of Fano resonances in the optical response (see the curve “1” in Fig. 2a). Thus, the topological vortical resonances with three different flavours Q_i acquire a mass $E_{g,Q_i}(q_i) = M_r(q_i)$, $i = 1, 2, 3$ when the mass term is coupled to the gauge fields. Now, we examine the stability of these states.

Let us numerically prove the coexistence of the Majorana-like modes with the anti-flavour ones in the following way. The precessing spin $\vec{\sigma}^{AB}(\vec{\sigma}^{BA})$ is no longer orthogonal to the valley currents $\vec{K}_B^{BA} + \vec{K}_A^{BA}$ ($\vec{K}_B^{AB} + \vec{K}_A^{AB}$) because

$$\vec{\sigma}^{AB} \cdot (\vec{K}_B^{BA} + \vec{K}_A^{BA}) \neq 0. \quad (24)$$

The spin precession (24) give rise nonzero values of the added mass with $m_{precession}$ (10) entering the mass term \tilde{M} (3),(5). As one can see in Fig. 4c, the effect of a nonzero value of $m_{precession}$ of the order of 0.0001 consists in a further flattening of one ($M_2(q)$) of the eigenvalues of the Majorana-like term with the replacement of one of the “wings” of the saddle by an “antiwing”. Thus, the spin–valley-current interaction restores the chiral symmetry of graphene charge carriers. The three resonances are chirality anomalies.

At large $m_{precession}$ of the order of 0.001, the eigenvalue $M_2(q)$ vanishes for all q except four wave numbers q_i , $i = 0, 1, 2, 3$ at which chirality anomalies remain in the form of three resonances with the flavours $Q(q_i) = \frac{(i+1)\pi}{4}$, $i = 1, 2, 3$ and one antiresonance with the antiflavour $Q(q_0) = -\frac{\pi}{4}$ (see Fig. 4d). It is important that the zero-energy Majorana-like mode itself with negative (positive) mass $Q(q_0)$, $Q(q_0) < 0$ ($Q(q_0) > 0$) as a mass of negatively (positively) charged graphene electrons (holes) has no physical meaning.

However, due to the electron–hole symmetry there always exists a superposition (mixture) of Majorana anti-pairs of vortex cores and chiral pairs of developed vortices with masses $M_1(q)$ and $M_2(q)$, respectively. Therefore, the $Q(q_0)$ can always be assigned to topological antidefects with a saddle-like dependence of the mass on \vec{q} in the vicinity of the $K'(K)$ antivalley.

Thus, the flavour interaction $\Sigma_{BA}\Sigma_{AB}$ ($\Sigma_{AB}\Sigma_{BA}$) render the vortical states massive as LH electron (RH hole) stable-vortices core with the flavour Q_n (antiflavour $-Q_n$), $n = 1, 2, 3$ acquire a mass $M_r(q_i) > 0$ ($-M_r(q_i) < 0$), $i = 1, 2, 3$ and the antimass $M_r(q_0) < 0$ ($-M_r(q_0) > 0$) is attributed to the RH electron (LH hole) unstable-vortex core with antiflavour (flavour) Q_0 .

The interaction $m_{\text{precession}}$, mediated by the precession caused by the quantum exchange, renders null the ability of the flavour interaction $\Sigma_{BA}\Sigma_{AB}$ ($\Sigma_{AB}\Sigma_{BA}$) to violate the chirality outside the graphene valleys for the LH electron (RH hole) vortex cores only. Then, our theory predicts that the flavoured vortex resonances will emerge at sufficiently low energies, when the law of topological-charge conservation precludes quantum interference through the annihilation of feathering with the Majorana zero-energy modes attributed to the mass-term eigenvalue $M_1(q)$. At high energies, both stable and unstable vortices develop, with topological charges of opposite sign; their total zero topological charge admits mutual quantum interference.

Now, one is able to construct associations between the concepts and terms of the Majorana scenario of admixing a sterile RH mass neutrino to three active mass LH neutrinos and the concepts and terms of the Majorana-like graphene physics.

In the absence of an electromagnetic field and, correspondingly, without electron–hole pairs, there exist three Majorana-like LH modes with positive electron (negative hole) masses $M_r(q_i)$ ($-M_r(q_i)$), $i = 1, 2, 3$ residing in the graphene sublattice A (B) and one RH Majorana-like antimode with a mass $M_r(q_0)$ of the opposite sign. The Majorana-like antimode can be attributed to the other sublattice B (A) and then it, as a real antimode, would be admixed to the real Majorana-like modes, remaining just as non-interacting (sterile) due to residing on the other sublattice because of chiral symmetry.

In a similar way, as in the flavoured graphene interaction, when neutrinos and electromagnetic plasma are decoupled, the three types of LH neutrinos (active neutrinos) are revealed explicitly in weak interactions and there also exists an RH neutrino of the 4th type (sterile neutrino, sterile RH lepton), which can be admixed without an additional resonance.

At low energies, when coupling takes place between electromagnetic fields and Majorana-like graphene modes of one sublattice A (B) only, without the antimode from the another sublattice B (A), the real flavour Majorana-like modes are exhibited through the Fano resonances. At higher energies, when the unstable high-energy antiflavour Majorana-like vortical state develops, quantum interference of all Majorana-like

vortical states occurs because of the overlap of all flavour and antiflavour graphene Dirac cones with each other. Similarly, in weak interactions, since the three active flavour neutrinos possess physical masses, the sterile neutrino, being periodically admixed, firstly, modifies the neutrino mass spectrum and, secondly, at high energies, by decolouring the neutrino beam, causes its components to interfere with each other, which gives rise to the three-flavour neutrino oscillations.

V. DISCUSSION AND CONCLUSION

So, according to the quasi-relativistic quantum-field theory of graphene Majorana-like fermions, zero-energy pseudo-Majorana modes reside in the Dirac point $K(K')$ of the graphene Brillouin zone as topologically nontrivial defects. Our approach elucidates physical meaning of the topological charge, the flavour of leptons is associated with the topological charge Q_i , $i = 0, 1, \dots$ of the vortex core.

The three Majorana-like flavour modes with repulsive interaction emerge in the graphene optical conductivity. The theoretical prediction of flavour Fano resonance with maximum of 4.74 eV (5.5×10^4 K) is in excellent agreement with maximum of 4.62 eV for an experimental ultraviolet graphene Fano interference which was registered earlier in [21]. The predicted resonances “F1” and “F2” being confirmed by the presence of the experimentally observed asymmetric UV spectrum line in the optical conductivity of graphene ensure that its value exceeds that predicted by the pseudo-Dirac model of graphene. For comparison, in other papers, the asymmetric peak “F2” is explained only phenomenologically as the existence of a weak coupling between photon scattering on Dirac-type graphene fermions with a continuous spectrum and the excitation followed by rapid decay of excitons with a discrete spectrum on flat regions in the vicinity of the M point of the Brillouin zone (see [22] and references therein). The *ab-initio* Green’s-function (GW) calculation, by fitting the so-called Fano resonance parameters, predicts the “F2” 780 meV bandwidth (exciton lifetime of the order of 0.5 fs) which is experimentally observed; but, the predicted excitonic 5.2 eV peak is blue-shifted relative to the experimental one. Conversely, the *ab-initio* GW–Bethe–Salpeter (GWBS) calculation, by fitting the Fano resonance parameters, predicts a close proximity of the excitonic peak to the “F2” peak (5.02 eV); but, the excitonic-peak bandwidth of the order of 200 meV corresponds to a slow excitonic decay (exciton lifetime of the order of 2.5 fs), which contradicts the excitonic instability in graphene. In Ref. [23], without elucidating the origin of the weak coupling between the two oscillators, a discrete level of a three-dimensional system with a quantum well with the attractive singular δ -potential type to the plane is used, phenomenologically incorporated into graphene, which yields a broadening equivalent to a rather slow decay, albeit faster in comparison with the excitonic one.

Both two eigenvalues $M_1(q)$ and $M_2(q)$ of the Majorana mass term \tilde{M} vanish at the Dirac points,

but in the neighborhood of the Dirac point, only one eigenvalue ($M_2(q)$) remains zero. The chirality of the topologically protected Majorana-like mode is violated by four resonances of the second mass-term eigenvalue $M_2(q)$. This chirality anomalies causes the electron (hole) conical Dirac bands to diverge. The four resonances can be considered as elementary excitations (quanta) of a certain flavour field. It has been proved that the degenerate zero-energy Majorana-like mode at the Dirac point $K(K')$ possesses zero total topological charge $Q = \sum_{n=0}^4 Q_i$. Under the condition that the cores of all vortical states reside in the valley $K(K')$, there are no prohibitions from the law of topological-charge conservation on the existence of quantum interference of the vortex featherings as the cause of the observed oscillations of the optical graphene conductivity in Fig. 2a.

Since the mass term opens a flavoured gap $E_{g,Q_i}(q_i)$, $i = 1, \dots, 4$ in the graphene bandstructure, the zero-energy Majorana-like modes become massive. Assigning spin and the corresponding topological charge to the flavour-field quanta, one obtains four flavour leptons. The three Majorana-like LH (RH) modes of them possess positive (negative) masses $M(q_i) = E_{g,Q_i}(q_i) > 0$, $i = 1, \dots, 3$ and participate in physical repulsive interactions with the preservation of chiral symmetry.

Since all vortical Majorana-like states are a superposition of the eigenstates of the Majorana mass term \tilde{M} , the unstable RH (LH) vortical Majorana-like state with the alternating-sign eigenvalue $M_1(q)$ is always admixed to the three-flavour chiral model outside the Dirac point, and, correspondingly, the mass $M(q_0) = E_{g,Q_0}(q_0) < 0$ ($M(q_0) = E_{g,Q_0}(q_0) > 0$) is always an attribute of the fourth non-chiral lepton, the interaction with which is suppressed by CP symmetry.

In our theory, the Majorana-like mixture of LH-chiral and RH-non-chiral vortical states when holding total zero topological charge is revealed through the quantum interference as three-flavour oscillations because the law of topological-charge conservation admits the redistribution of the energy among the flavoured constituents of the flavourless composition.

We offer a Majorana scenario of three-flavour mass-neutrino oscillations by drawing parallels and interpreting the phenomenological mixing of LH active neutrinos with an RH sterile lepton as the formation of a bandstructure gap by means of the interaction of nonzero topological charges of Majorana-like modes. A necessary and sufficient condition for this scenario is the existence of such Majorana modes with topological charges of opposite sign which reside on different sublattices. The predicted aperiodic variation of the optical graphene response for the mixed Majorana-like state explains the three-flavour neutrino oscillations. Within the framework of the proposed toy model, these oscillations can be interpreted as the existence of a sterile $M(q_0)$ -mass RH antiflavour neutrino, periodically admixed to the three chiral LH active neutrinos

with real physical flavours. The all flavours are different topological charges Q_n , $\sum_n Q_n = 0$.

-
- [1] I. Esteban, M.C. Gonzalez-Garcia, M. Maltoni, T. Schwetze, A. Zhou. The fate of hints: updated global analysis of three-flavour neutrino oscillations. *JHEP*. **2020**, 178 (2020).
 - [2] M. Escudero. Neutrino decoupling beyond the Standard Model: CMB constraints on the Dark Matter mass with a fast and precise N_{eff} evaluation. *J. Cosmol. Astropart. Phys.* **2019**, 007 (2019).
 - [3] T. Binder, M. Garny, J. Heisig, S. Lederer, K. Urban. Excited bound states and their role in dark matter production. *Phys. Rev. D*. **108**, 095030 (2023).
 - [4] I. Esteban, M.C. Gonzalez-Garcia, A. Hernandez-Cabezudo. Global analysis of three-flavour neutrino oscillations: synergies and tensions in the determination of θ_{23} , δ_{CP} , and the mass ordering. *JHEP*. **2019**, 106 (2019).
 - [5] J. de Vries, H.K. Dreiner, J. Groot, J.Y. Günther, Z.S. Wang. Probing light sterile neutrinos in left-right symmetric models with displaced vertices and neutrinoless double beta decay. *J. High Energy. Phys.* **2025**, 7 (2025).
 - [6] K. Chaturvedi. Study of sterile neutrino contribution to neutrinoless double beta decay. *SCIREA J. Phys.* **9**, 130 (2024).
 - [7] C. Adams *et al.* (NEXT Collaboration). The NEXT-100 Detector. *Eur. Phys. J. C*. **86**, 114 (2026).
 - [8] M.A. Acero *et al.* White paper on light sterile neutrino searches and related phenomenology. *J. Phys. G Nucl. Part. Phys.* **51**, 120501 (2024).
 - [9] G. Gagliardi, C. Köhler, T. Lasserre, S. Mohanty, X. Stribl, The KATRIN Collaboration. Sterile-neutrino search based on 259 days of KATRIN data. *Nature*. **648**, 70 (2025).
 - [10] H.-Y. Ren, Y.-N. Ren, Q. Zheng, J.-Q. He, L. He. Electron-electron interaction and correlation-induced two density waves with different Fermi velocities in graphene quantum dots. *Phys. Rev. B*. **108**, L081408 (2023).
 - [11] H. Grushevskaya, G. Krylov. Two-Dimensional Braiding of Two-Dimensional Majorana Fermions : Manifestation in Band Structure of Graphene. *Int J. Nonlin. Phen. Compl. Sys.* **22**, 41 (2019).
 - [12] J. Zak. Berry's phase for energy bands in solids. *Phys. Rev. Lett.* **62**, 2747 (1989).
 - [13] D. Vanderbilt, *Berry Phases in Electronic Structure Theory: Electric Polarization, Orbital Magnetization and Topological Insulators*, (Cambridge University Press, Cambridge, 2018).
 - [14] Y. Huang, Y. Liu, M. Wang, X. Chen, H. Han, A. Yu, G.P. Wang. Topological transition of Pancharatnam–Berry phase in a nonlocal twisted bilayer metasurface. *Scientific Reports*. **15**, 11182 (2025).
 - [15] D.J. Griffiths, D.F. Schroeter. *Introduction to Quantum Mechanics*, third edition. (Cambridge University Press, Cambridge, 2018)
 - [16] H. Grushevskaya, G. Krylov. Vortex Dynamics of Charge Carriers in the Quasi-Relativistic Graphene Model: High-Energy $\vec{k} \cdot \vec{p}$ Approximation. *Symmetry*. **12**, 261 (2020).
 - [17] H.V. Grushevskaya, G.G. Krylov. Magneto-optical anomalies and Majorana-like fermion interactions in graphene. *Int J. Nonlin. Phen. Compl. Sys.* **28**, 144 (2025).
 - [18] H.V. Grushevskaya, G.G. Krylov. Chapter 9. Electronic Structure and Transport in Graphene: QuasiRelativistic

Dirac-Hartree-Fock Self-Consistent Field Approximation. In: *Graphene Science Handbook: Electrical and Optical Properties*. Vol. 3. Chapter 9. Eds. M. Aliofkhazraei *et al.* (Taylor and Francis Group, CRC Press, USA, UK, 2016). Pp.117-132.

- [19] H.V. Grushevskaya, G. Krylov. Semimetals with Fermi Velocity Affected by Exchange Interactions: Two Dimensional Majorana Charge Carriers. *J. Nonlin. Phenom. in Complex Sys.* **18**, no. 2, 266-283 (2015).
- [20] H.V. Grushevskaya, G. Krylov, V.A. Gaisyonok, D.V. Serov. Symmetry of Model $N = 3$ for Graphene with Charged Pseudo-Excitons. *Int. J. Nonlin. Phenom. in Complex Sys.* **18**, no. 1, 81-98 (2015).
- [21] K.F. Mak, J. Shan, T.F. Heinz. Seeing many-body effects in single- and few-layer graphene: Observation of two-dimensional saddle-point excitons. *Phys. Rev. Lett.* **106**, 046401 (2011).
- [22] K.F. Mak, L. Ju, F. Wang, T.F. Heinz. Optical spectroscopy of graphene: From the far infrared to the ultraviolet. *Solid State Com.* **152**, 1341 (2012)
- [23] R. O. Kuzian, D. V. Efremov, E. E. Krasovskii. Fano physics behind the N-resonance in graphene. *Phys. Rev. Res.* **7** 013180 (2025.).